

Fabrication and Self-Assembly of Hydrophobic Gold Nanorods

Koji Mitamura,[†] Toyoko Imae,^{*,‡} Nagahiro Saito,[†] and Osamu Takai^{*,‡,§}

Graduate School of Engineering and Ecotopia Science Institute, Nagoya University, Chikusa, Nagoya 464-8603, Japan, and Graduate School of Science and Technology, Keio University, Hiyoshi, Yokohama 223-8522, Japan

Received: March 31, 2007; In Final Form: May 25, 2007

Hydrophobic gold nanorods were fabricated from hydrophilic gold nanorods coated with hexadecyltrimethylammonium bromide by treating with mercaptopropyltrimethoxysilane (MPS) and subsequently octadecyltrimethoxysilane (ODS). The fabrication of the hydrophobic shell went through the process of (1) binding MPS onto the nanorods, (2) hydrolysis of methoxysilanes, and (3) immobilization of ODS by dehydration condensation. The 2- or 3-D ordered structures of hydrophobic nanorods were self-assembled by the evaporation of solvent on a substrate. The aspects of 2-D assemblies were dependent on the concentration of the nanorods, as was seen in transmission electron microscopic images. At a low concentration, the nanorods assembled parallel to the substrate, whereas they stood on the substrate at a high concentration. On the other hand, in a solid of the gold nanorods, the formation of the 3-D assembly was confirmed by small-angle X-ray scattering. The assembly consisted of hexagonal arrays of the gold nanorods and their lamellar accumulation.

Introduction

Metallic or semiconductive nanoparticles are used as inks, catalysts, biosensors, and electromagnetic devices in the industrial and medical fields. The characters of such nanoparticles are based on quantum effects.¹ To develop their further functionalities, recently nanoparticles with various shapes were synthesized. The nanocolloids with nonspherical shapes such as nanowires,² nanocubes,³ hexagons,^{4–6} triangles,^{7,8} and crowns⁹ display anisotropic behavior in optical and electric properties, which differ from spherical nanoparticles. As one such nanoparticle, nanorods are focused since their properties depend on their transversal and longitudinal sizes.¹⁰

Many investigations have been performed for industrial and medical utilization of anisotropic gold nanorods.^{11–13} For instance, the nanorods direct their application as a memory medium by utilizing transformation from rods to spheres under irradiation of near-IR rays.¹⁴ Furthermore, the gold nanorods can be used as an antineoplastic agent.¹¹ When transformation of gold nanorods occurs, thermal energy is generated, and cancer cells are eradicated with the consequent energy. In addition, the anisotropy of nanorods facilitates their self-assembly or ordering. Although the self-assembly of gold nanorods has been reported, such investigations have been performed for water-dispersed nanorods.^{15–17} The use of water dispersions is because gold nanorods are synthesized in an aqueous phase.^{6,18–20} The surface modification of gold nanorods with chemicals is difficult owing to protection by hexadecyltrimethylammonium bromide (CTAB) molecules, which strongly attach to the nanorod surface during their preparation.

In industrial conditions where water is unusable, the assembly of water-dispersed nanorods is not necessarily preferential, but

that of hydrophobic or lipophilic nanorods is suitable. In spite of such a requirement, reports on the hydrophobation of gold nanorods are few: the modification was carried out by electrostatic binding of a hydrophobation agent (tetraoctylammonium bromide) on a mercaptosuccinic acid-modified gold nanorod²¹ and covalent binding of a hydrophobation agent (octadecyltrimethoxysilane (ODS)) on a silica-modified nanorod that was prepared by treatment with tetraethoxyorthosilane (TEOS) after being wrapped by three kinds of polyelectrolytes.²² In these procedures, the shell on the nanorod core was formed by noncovalent binding²¹ or it was thick.²² Thus, in the present work, a new method for the hydrophobation of gold nanorods was proposed to prepare a chemically stable and thin organosilane shell by using mercaptopropyltrimethoxysilane (MPS) as a linker and ODS as the hydrophobation agent. Furthermore, ordered assembly formation by the resulting nanorods was demonstrated.

Experimental Procedures

Materials. All chemicals were commercially available and used without further purification. Ultrapure water ($<0.054 \mu\text{S}$) was used through all the experiments.

Preparation of Gold Nanorods. Gold nanorods were prepared at 30 °C by a seed-mediated method.¹⁹ A seed solution was prepared as follows: a freshly prepared aqueous solution (0.016 cm³) of 0.01 M NaBH₄ was added dropwise into a yellow aqueous solution (0.3 cm³) of 0.25 mM HAuCl₄ and 0.095 M CTAB with mild stirring. The preparation of a growth solution is as follows: an aqueous solution (0.013 cm³) of 0.01 M AgNO₃ and an aqueous solution (0.15 cm³) of 0.1 M ascorbic acid were mixed with a yellow aqueous solution (20 cm³) of 0.5 mM HAuCl₄ and 0.095 M CTAB under mild stirring. At the next step, the brown seed solution was mixed with the transparent growth solution, and the mixture was kept for at least 12 h, where a brownish red solution was obtained.

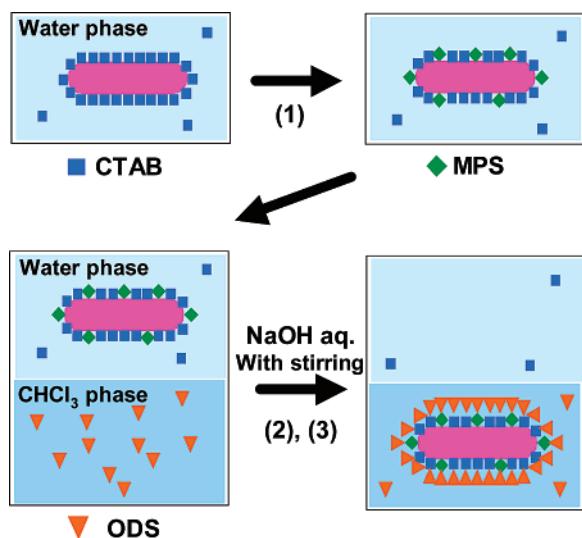
Hydrophobation of Gold Nanorods. The excess CTAB in an aqueous dispersion (3.0 cm³) of as-prepared gold nanorods

* Corresponding authors. (T.I.) Tel./fax: +81-45-566-1799; e-mail: imae@educ.cc.keio.ac.jp. (O.T.) Tel./fax: +81-52-789-3259; e-mail: takai@esi.nagoya-u.ac.jp.

[†] Graduate School of Engineering, Nagoya University.

[‡] Keio University.

[§] Ecotopia Science Institute, Nagoya University.

SCHEME 1. Illustration of Surface Modification of Gold Nanorods^a


^a (1) Binding of MPS, (2) hydrolysis of organosilanes, and (3) dehydration condensation.

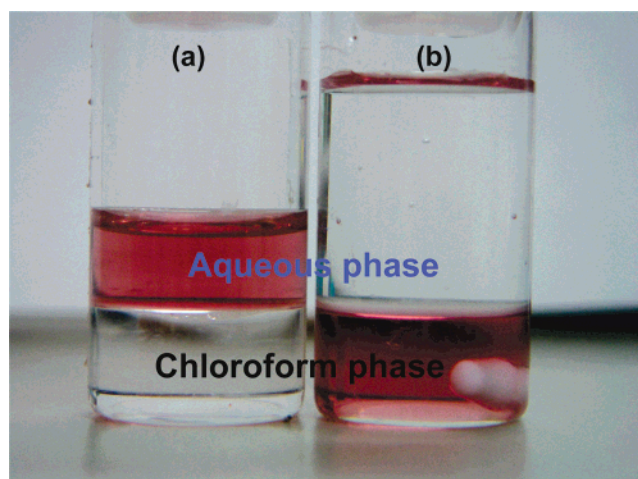


Figure 1. Visual observation of hydrophobation reaction. (a) Before and (b) after.

was removed by centrifugation and a following extraction with chloroform (gold nanorod dispersion/chloroform = 2:1 (v/v)). After discarding the chloroform phase, an ethanol solution (30 mm³) of 10 mM MPS was added to the excess CTAB-free gold nanorod dispersion, and the mixture was vigorously stirred for 30 min. Subsequently, a chloroform solution (3.0 cm³) of ODS and an aqueous solution (30 mm³) of 1 N NaOH were added to this mixture. After that, the two-phase system was vigorously stirred. During stirring for at least 3 h, the color of the aqueous phase was transferred to the organic phase, which involved turbidity. The organic phase was collected and washed 3 times with water. After the solvent was exchanged to hexane by evaporation, the dispersion was kept in a freezer (-4 °C), followed by precipitation of the gold nanorods. After the decantation, the precipitates were redispersed into hexane or chloroform. The processes of precipitation and redispersion were repeated 4 times.

Measurements. TEM observations were carried out on a JEM-2500TS. The samples were prepared by evaporating solvent from a dispersion (5 mm³) of nanorods on a carbon-deposited copper grid. IR absorption spectroscopic characterizations were carried out by a DIGILAB FTS-7000. Chloroform

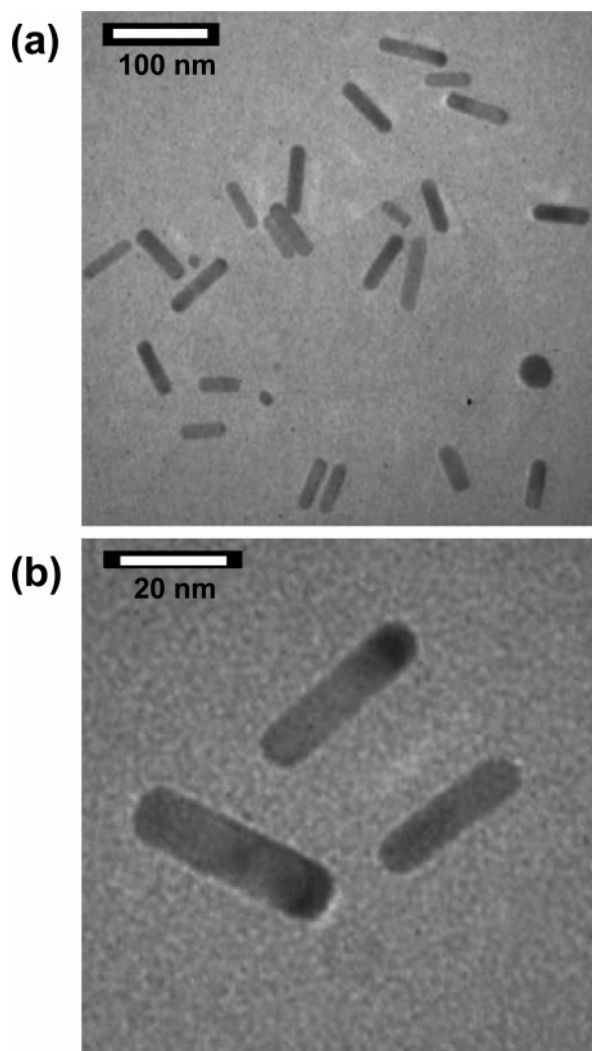


Figure 2. TEM images of hydrophobic gold nanorods (in hexane, at a low (dilute) concentration). (a) At low magnification and (b) at high magnification.

solutions of analytes (10 mM for MPS, ODS, and CTAB) and a chloroform dispersion of ODS-modified gold nanorods were dried on a KBr window. UV-vis absorption spectra were taken by a Simadzu UV-3600 spectrometer using a quartz cell (1 cm path) for the diluted solutions down to adequate concentrations where the absorbance was below the detection limit. Absorbance at 803 nm was used as a measure of the nanorod concentration in a dispersion. Small-angle X-ray scattering (SAXS) was measured on a Rigaku instrument (SAX-LPB) at a 1 m camera length, equipped with an X-ray source of Cu-K α radiation (wavelength of the X-ray, $\lambda = 0.154$ nm). The scattered X-rays were recorded on an imaging plate, and the intensity was averaged around each scattering angle. The experimental range of the scattering vector ($Q = 4\pi\sin(\theta/2)/\lambda$, where θ is the scattering angle) was 0.08–2.0 nm⁻¹. A nanorod dispersion (5 cm³, absorbance 3.15 at 803 nm) was poured into a glass capillary (2 mm diameter), and the solvent was evaporated at ambient conditions. Then, the resulting solid of gold nanorods displayed a metallic luster and could be redispersed in hexane.

Results and Discussion

Fabrication of Hydrophobic Gold Nanorods. Hydrophobation of gold nanorods was performed by the treatment of CTAB-coated gold nanorods with MPS and ODS in a two-phase

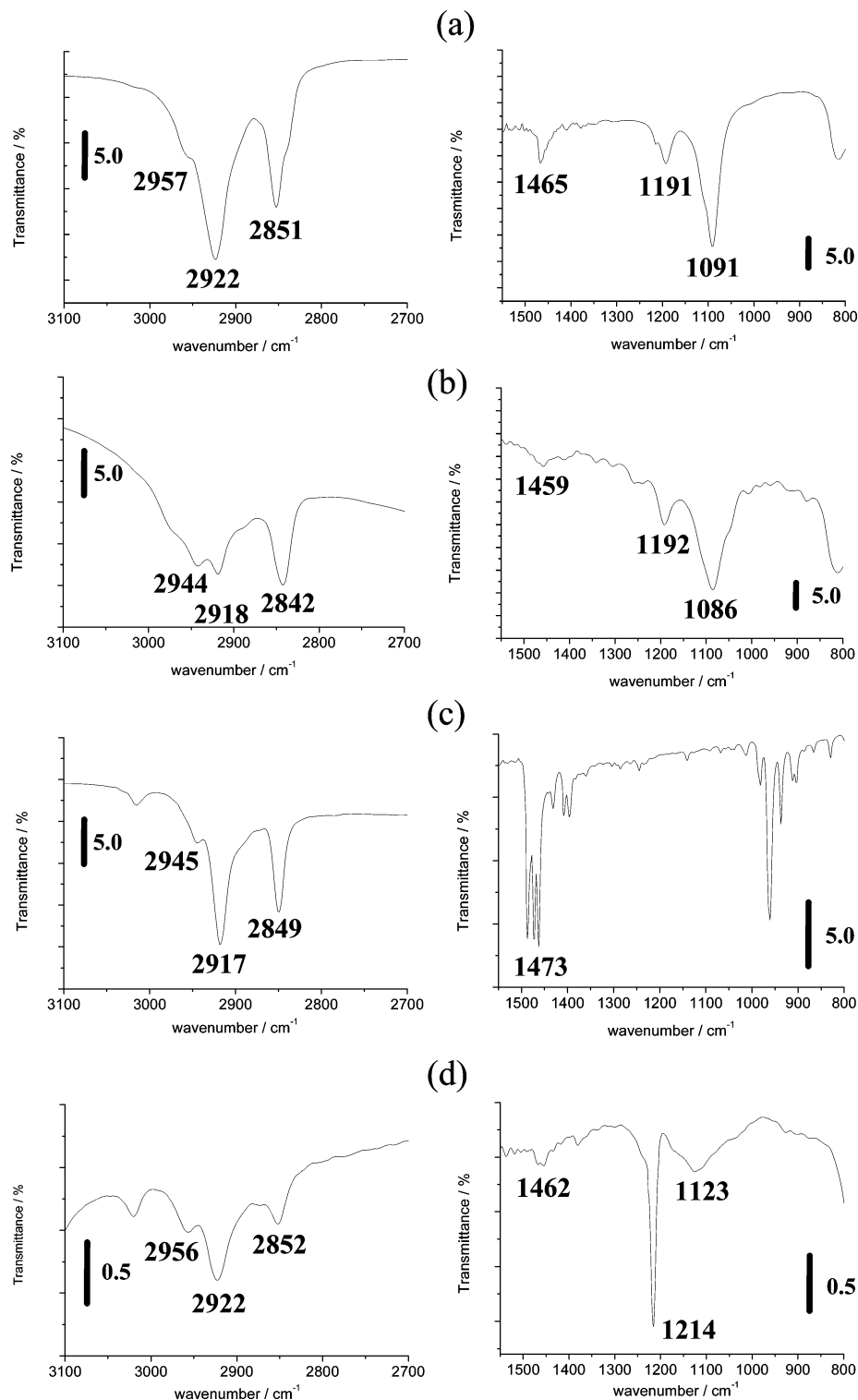


Figure 3. IR spectra of (a) ODS, (b) MPS, (c) CTAB, and (d) ODS-modified gold nanorods.

system (water and chloroform). The process for the formation of the organosilane shell on CTAB-coated gold nanorods consists of three kinds of reactions, that is (1) binding of MPS onto the nanorods, (2) hydrolysis of methoxysilane (Si-OR), and (3) immobilization of ODS by a dehydration condensation (polymerization among organosilanes) (Scheme 1). As shown in Figure 1, the nanorods were transferred from an aqueous phase into a chloroform phase, after the process was over. Then, the immobilization of ODS molecules as a hydrophobator on the gold nanorods was required for the production of hydrophobic gold nanorods since the CTAB-capped gold nanorods

(both with and without MPS treatment) in the absence of ODS were not transferred to an organic solvent.

The resulting nanorods (aspect ratio 3.3 ± 0.3) were individually isolated, and no coagulation of the nanorods was observed using TEM (Figure 2), indicating stable dispersion at a dilute condition. It is also notable that the shell structure around the ODS-modified nanorods was too thin in thickness to be visible on TEM images since the ODS molecules bound on the nanorods as a monolayer. This situation is different from two reports on silica-coated gold nanorods.^{22,23} Since the nanorods were fabricated by a silane coupling reaction of TEOS on

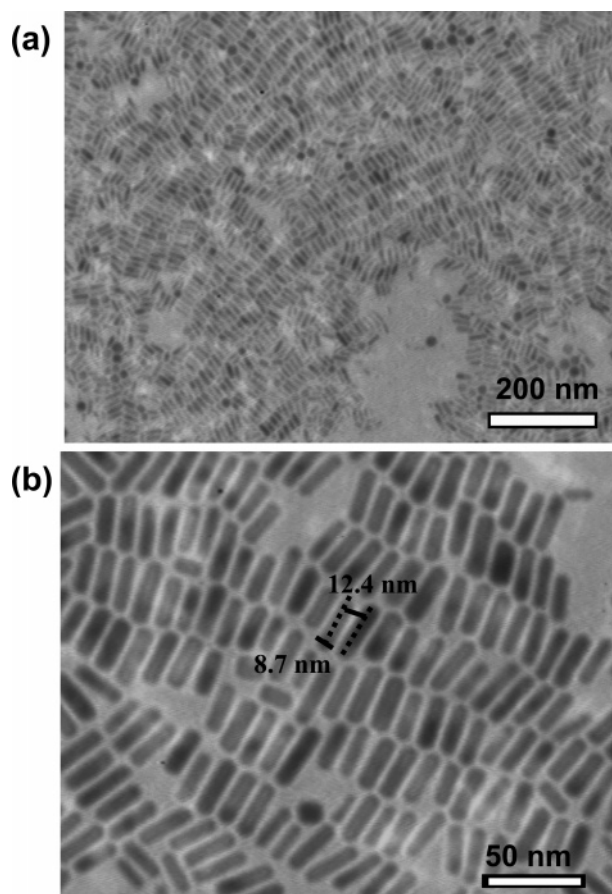


Figure 4. TEM images of assemblies of hydrophobic gold nanorods (in hexane, at a medium concentration). (a) At low magnification and (b) at high magnification.

polyelectrolyte shell or of sodium silicate on a MPS shell, their shells (former: >12 nm and latter: 5–7 nm) were thick enough to be visualized on TEM.

In this hydrophobation of gold nanorods, the hydrophobic nanorods ($[CTAB] = \sim 2.0$ mM and $[Au] = 0.5$ mM) were obtained after single centrifugation and extraction by chloroform (see Experimental Procedures). However, without any removal of CTAB ($[CTAB] = 95$ mM and $[Au] = 0.5$ mM), the nanorods were not transferred to an organic solvent. This was not due to binding of MPS on gold nanorods (corresponding to the absence of reaction 1 in Scheme 1) because excess (free) CTAB prevented the binding reaction of MPS. On the other hand, at a low CTAB concentration ($[CTAB] = \sim 0.16$ mM and $[Au] = 0.5$ mM) after double cycles of centrifugation and extraction, the color of the organic phase clearly became blue, indicating aggregation of the gold nanorods. Namely, the protection capacity of CTAB at a low CTAB concentration was too low to disperse the nanorods in any solvents. From these facts, it is clear that an adequate (minimized) amount of a CTAB bilayer, so as to maintain the hydrophilicity of nanorods and replace them with MPS, is crucial to the hydrophobation of the nanorods.

The presence of OH^- ions is also essential to the hydrophobation of the nanorods (see Experimental Procedures). Without the addition of a NaOH solution, hydrophobation did not occur even after 1 day. Moreover, even when an aqueous HCl solution was added instead of an aqueous NaOH solution, transfer to the organic phase was not observed. The difference between alkaline and acidic conditions comes from distinct characters in their catalytic action. Both hydroxyl ions and protons promote

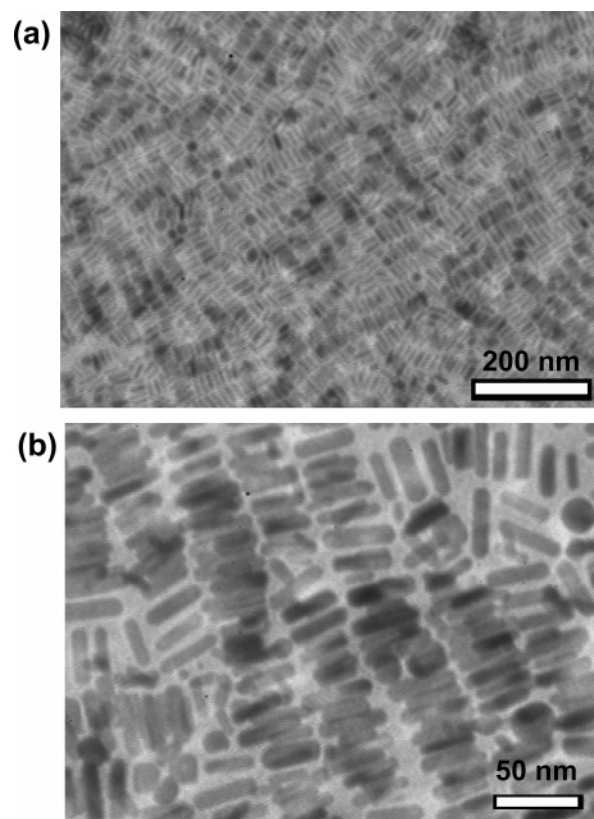


Figure 5. TEM images of assemblies of hydrophobic gold nanorods (in hexane, at a high concentration). (a) At low magnification and (b) high magnification.

the hydrolysis of Si-OR groups, corresponding to step 2 in Scheme 1. However, the promotion is more intensive by the former than the latter. Thus, such intensive hydrolysis at alkaline conditions caused efficient dehydration condensation among organosilanes (MPS and ODS) for the hydrophobation.

As-prepared hydrophobic gold nanorods were purified by cooling the nanorod dispersion at -4 °C. Then reddish precipitates of the nanorods were separated due to the lesser solubility of organic components on the nanorods. Since free ODS is dissolved in hexane and chloroform even at -4 °C, excess ODS remains in the supernatant. After the purification process was repeated 4 times, the resulting gold nanorod precipitates were redispersed in nonpolar organic solvents such as hexane, chloroform, and toluene without any precipitation at room temperature. Moreover, the nanorods were neither dispersed nor transferred to the water phase. These results indicate that the amount of ODS strongly bound on the gold nanorods is large enough to isolate the nanorods in the organic phase.

The process of siloxane bonding in the present system was confirmed from IR spectra of ODS-modified gold nanorods after purification procedures in comparison with those of ODS, MPS, and CTAB, as shown in Figure 3. The ODS molecules displayed characteristic bands at 2957, 2922, 2851, and 1465 cm^{-1} , which were attributed to the antisymmetric stretching vibration of the CH_3 groups and to the antisymmetric stretching, symmetric stretching, and bending vibrations of the CH_2 groups, respectively. These bands were common to the spectra of MPS, CTAB, and ODS-modified gold nanorods.

Additionally, ODS and MPS possessed IR bands at 1191 and 1091 cm^{-1} , which were assigned to the CH_3 rocking and SiO–C stretching modes of Si–O– CH_3 respectively.^{24,25} However, ODS-modified gold nanorods displayed sharp and broad bands

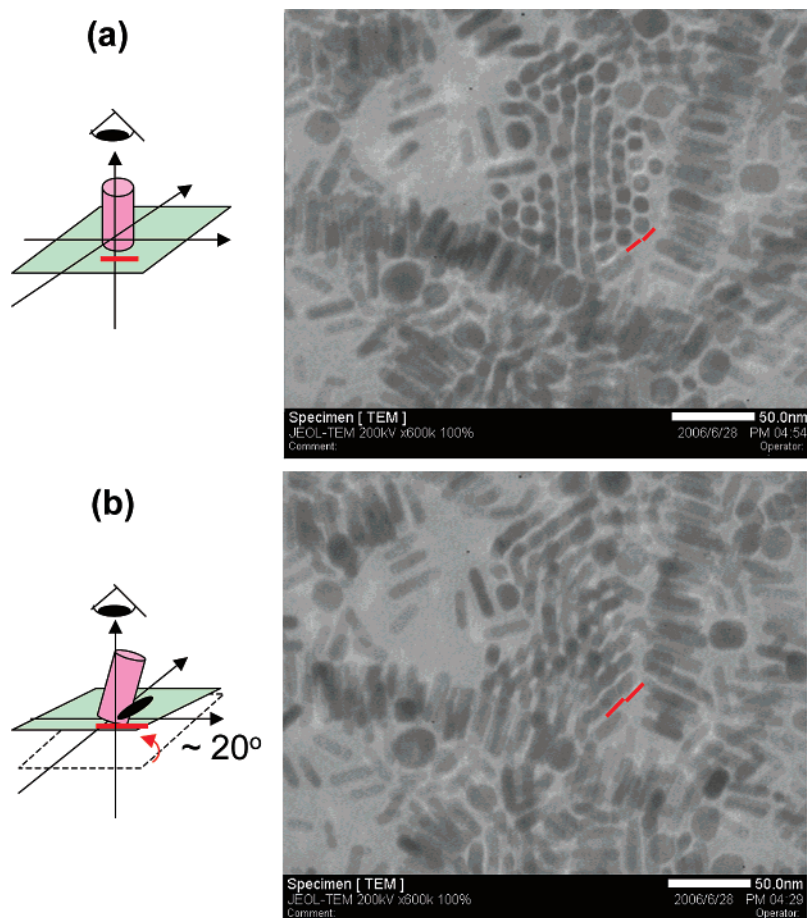


Figure 6. TEM images of assemblies of hydrophobic gold nanorods (in hexane, at a high concentration). (a) Without tilt of a grid and (b) with tilt of a grid.

at 1214 and $\sim 1123\text{ cm}^{-1}$, respectively, in the same wavenumber region. The observed characteristic bands of ODS-modified gold nanorods remained in the same intensity scale even after a further 4 times of purification. Since the 1214 and $\sim 1123\text{ cm}^{-1}$ bands appeared instead of bands of Si-O-CH₃, they were assigned to vibration bands (stretching modes) of Si-O-Si, which are a product of dehydration condensation. Incidentally, the corresponding bands have been reported in a similar region ($950\text{--}1150$,²⁴ 1033 ,²⁵ 1136 , and 1049 cm^{-1}).²⁶ Since an Si-O stretching vibration band of Si-O-H at 900 cm^{-1} was not observed as well as bands of Si-O-CH₃ not being observed, it is suggested that there are no free Si-OH groups and, moreover, that all MPS and ODS interact through siloxane linkages. It is noticed that direct binding of ODS with MPS and lateral binding between ODS molecules on gold nanorods through a dehydration condensation reaction is a main motivating force for the immobilization of ODS on gold nanorods.

The formation of hydrophobic gold nanorods has been carried out by two groups.^{21,22} In the ref 21, hydrophobic gold nanorods were prepared by electrostatic interactions between mercaptosuccinic acid-modified gold nanorods and hydrophobation agents. The method is simple, but the fear is the release of hydrophobation agents from the nanorods. In the ref 22, although the hydrophobation agents covalently attached to gold nanorods via a silane coupling reaction, the gold nanorods had to undergo cumbersome procedures such as the deposition of three polyelectrolytes (polystyrene sulfonate, polyallylaniline hydrochloride, and poly(vinylpyrrolidone)) on the nanorods and silica coating by TEOS. In the present study, the hydrophobation of gold nanorods was performed in two steps (binding steps of MPS and ODS) as shown in Scheme 1. Moreover, the ODS

molecules were strongly covalently bonded on the nanorods abundantly enough to disperse them in an organic medium. The present preparation procedure is advantageous over the utilization of gold nanorods from the viewpoint of simple preparation, easy purification paths, and strong attachment of hydrophobation agents as a thin shell on the gold nanorods.

Self-Assembly of Hydrophobic Gold Nanorods. It has been reported that hydrophobic inorganic semiconductor nanorods formed an ordered structure at the air-water interface.²⁷ However, there is no report on 2- or 3-D ordered structures of hydrophobic gold nanorods. Thus, in the present work, assembly formation of the hydrophobic gold nanorods was attempted. First, the nanorods were disorderly dispersed and individually isolated in a TEM image of a specimen prepared from a dispersion in hexane at a low (dilute) concentration (absorbance of the nanorod at $803\text{ nm} = 0.16$) (see Figure 2). On the other hand, with the increase in nanorod concentration (absorbance of the nanorod at $803\text{ nm} = 3.15$), the recumbent nanorods were organized in 2-D like bedded tiles, as seen in the TEM images (Figure 4). Furthermore, at a high concentration of nanorods (absorbance of the nanorod at $803\text{ nm} = 25.2$), the 2-D assemblies (Figure 5) could be observed similar to those shown in Figure 4. However, the defect region of the 2-D array in Figure 5 became smaller than that in Figure 4, and the area of the assembly enlarged from a few hundred nanometer order at a medium concentration to a sub-micrometer order at a high concentration. Additionally, in Figure 5, the accumulation of nanorods on the nanorod sheet was observed with frequency.

At a high concentration, another type of assembly was also observed. The cross-sections of TEM images marked with lines in Figure 6a at a tilt angle of 0° were circular, and this feature

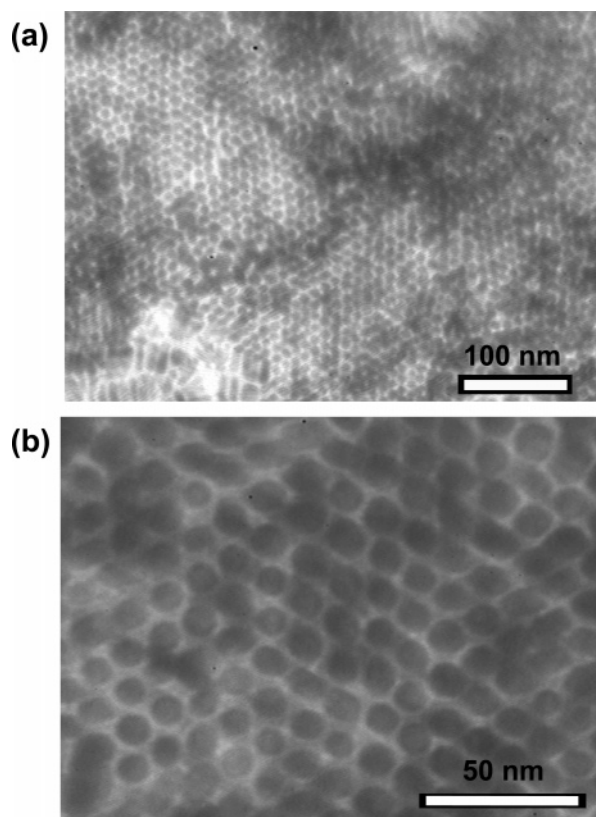


Figure 7. TEM images of highly ordered hydrophobic gold nanorods (in hexane, at a high concentration). (a) At low magnification and (b) at high magnification.

changed to an ellipsoidal structure, as marked with lines in Figure 6b, when the grid was tilted at an angle of $\sim 20^\circ$. It is interpreted that the nanorods are vertically arranged to a substrate, that is, they are standing on the substrate. At a high concentration, while the recumbent nanorods as shown in Figure 5 were abundant, the nanorods were at times vertically assembled in large domains of a sub-micrometer order as shown in Figure 7.

In vertical assembly of the nanorods, they arranged in a hexagonal packing array, as is seen clearly in Figure 7b, and the average center-to-center distance between the closest adjacent nanorods was 13.0 nm. This distance is larger than the averaged diameter of the nanorods, 8.7 nm (see Figure 4). The difference (~ 4.3 nm) between these sizes is due to the presence of an organic shell on the nanorods, but it is shorter than the calculated shell thickness (maximum of 6.8 nm) since the calculated lengths of CTAB and ODS are 2.1 and 2.6 nm, respectively. The alkyl chains could be interdigitated and/or tilted, as observed in the assembly of nanoparticles protected with hydrophobic alkyl chains.^{28,29} On the other hand, the center-to-center distance (13.0 nm) in crystal-like hexagonal packing is close to the distance (12.4 nm) between the 2-D ordered nanorods (see Figure 4). This implies that the closest rod-rod distance is maintained even in the 2-D assembly by an attractive interaction.

The interaction between nanorods can be caused by the induced dipole moment in addition to the steric hindrance. The induced dipole moment is generated by the instantaneous polarization or fluctuation of electron density in the nanorod, and it induces the oppositely directed polarization in the adjacent nanorod. Consequently, the dipole-dipole interaction was generated between adjacent nanorods. In that case, the side-by-side interaction is more preferential than the edge-to-edge

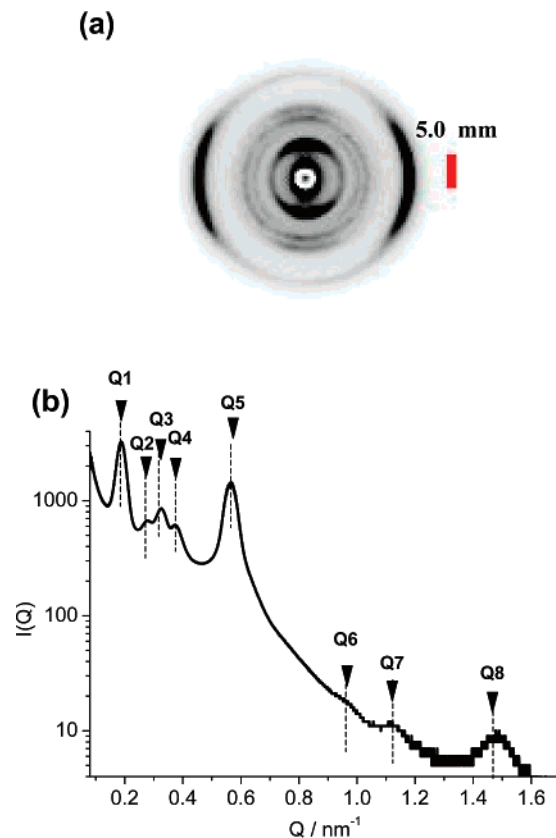


Figure 8. (a) Diffraction pattern and (b) scattered X-ray intensity-scattering vector profile obtained from the assembly of hydrophobic gold nanorods (in hexane, at a high concentration).

one since the induced dipole moments can be more effectively compensated in the former type. In fact, in all the assemblies observed (Figures 4–7), the adjacent nanorods had contact with their sides.

A similar side-by-side interaction has been observed for alkyl-modified (hydrophobic) BaCrO_4 nanorods, and it was concluded that the BaCrO_4 nanorods could be self-assembled via the interdigitation of alkyl chains on the nanorods and the van der Waals force (including the interaction between dipole moments) between nanorods.²⁸ However, an assembly of gold nanorods modified by a thiol compound (mercaptopropionic acid (MPA)) in an aqueous dispersion was formed via an edge-to-edge interaction between the nanorods (hydrogen bonds between carboxyl groups in MPA molecules), due to the preferential adsorption of MPA on the edge of the nanorods.^{30,31} A side-by-side interaction between nanorods was more preferred in the present case since the organosilanes attached to the whole nanorod surface. This situation is clearly different from the assembly consisting of thiol-modified hydrophilic gold nanorods.

2-D assemblies as seen in Figures 4–7 provide the possibility that the hydrophobic gold nanorods form highly ordered assemblies in bulk (namely, in a solid state). Such a structure was revealed by SAXS measurements for the nanorod solid. After solidification, the diffraction arcs were observed in the 2-D scattering image shown in Figure 8a. Additionally, they were localized depending on the scattering vector \mathbf{Q} (the direction and absolute value). This anisotropic SAXS pattern indicates that the assembly of the nanorods displaying the macroscopically ordered structure was formed inside the solid.

The averaged intensity-scattering vector ($\mathbf{Q} = |\mathbf{Q}|$) profile is shown in Figure 8b. From each \mathbf{Q} value of the Bragg peaks (Q1–Q8) in the reciprocal space, the spacing lengths (d) of

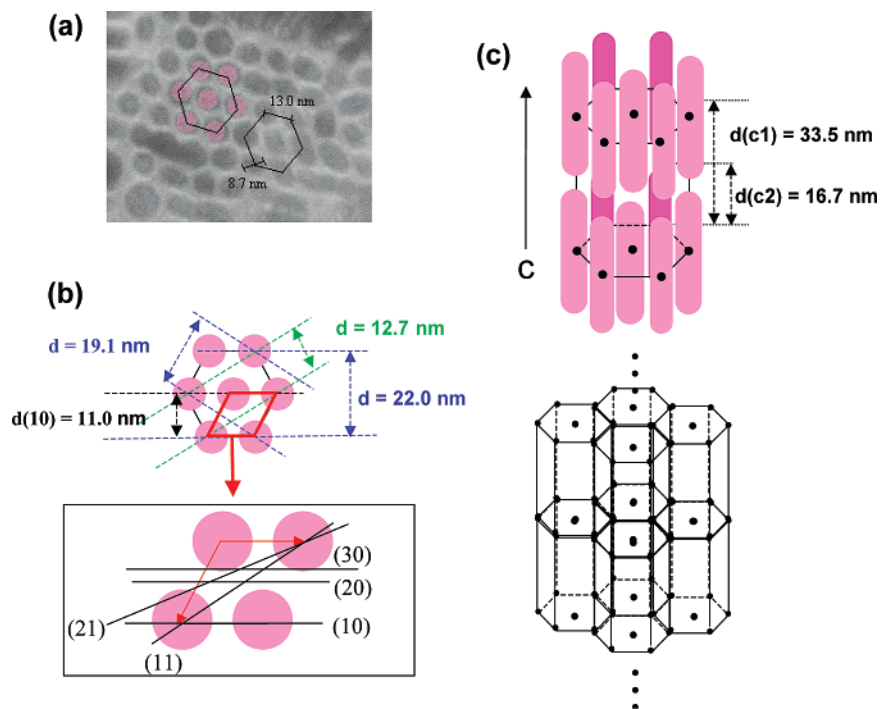


Figure 9. (a) TEM image and illustration of hexagonal packing of standing nanorods, (b) hexagonal lattice and its monoclinic unit in a 2-D array, and (c) 3-D lamellar accumulation of hexagonal array.

TABLE 1: Q Values of Bragg Peaks Q1–Q8 Denoted in Figure 8 and d Values Evaluated from Each Q Value and Calculated on the Basis of Hexagonal Packing (Figure 9)

Q	exptl Q value (nm^{-1}) (d value (nm))	d value (nm) calculated on basis of hexagonal packing (diffraction plane ^a)
Q1	0.189 (33.2)	33.0 (c1)
Q2	0.284 (22.0)	22.0 ^b
Q3	0.325 (19.3)	19.1 ^b
Q4	0.377 (16.6)	16.5 (c2)
Q5	0.567 (11.0)	11.0 (10) and (c3)
Q6	0.981 (6.4)	6.4 (11)
Q7	1.128 (5.6)	5.5 (20)
Q8	1.486 (4.2)	4.2 (21 and/or 30)

^a Notation of hexagonal model and diffraction plane is described in Figure 9b,c. ^b These distances correspond to those shown in Figure 9b.

repeating units in the structure were evaluated by using Bragg's equation ($2d \sin(\theta/2) = n\lambda$). The d values are listed in Table 1. When the hexagonal packing (Figure 9a) is indexed as shown in Figure 9b, the peaks Q5–Q8 correspond to spacings of the (10), (11), (20), and (21 and/or 30) planes, respectively. Peaks Q2 and Q3 also come from the spacing of hexagonal packing (see Figure 9b). Apart from such a hexagonal model, when orthorhombic models were applied in the analysis, no agreement with the X-ray profile could be obtained. Thus, from these evaluations, it was confirmed that the assembly in bulk took a hexagonal structure.

Q1 can be assigned to the repeating distance along the long axis of the nanorod (c -axis in Figure 9c) since the spacing length (33.2 nm) evaluated from the Q1 peak is comparable to the summation of the averaged longitudinal length of the nanorod (28.7 nm) and the organic shell thickness of the alkyl chains (~ 4.3 nm) from TEM observations. This spacing in the c -axis is denoted as $c1$. The Q4 peak is notated as $c2$ since the spacing length (16.6 nm) from Q4 is half of the repeating distance along the long axis of the nanorod. The $c3$ peak should appear at $\sim 0.57 \text{ nm}^{-1}$ (comparable to ~ 11.0 nm), but it is overlapped

by the Q5 peak (0.567 nm^{-1}) from hexagonal packing. Since these diffraction peaks (Q1 and Q4) satisfied the Bragg equation at $n = 1$ and 2, respectively, along the longitudinal direction of the gold nanorods, it was found that the nanorods formed a lamellar accumulation of hexagonal arrays (see Figure 9c). In the assembly, the center-to-center distance (12.7 nm) calculated from the SAXS results was consistent with the value (13.0 nm) from the TEM observation (Figure 9) and that (12.4 nm) in the 2-D array (Figure 4). These results indicate that the (dipole–dipole) interaction between nanorods in the 2-D assembly is common to that in the 3-D assembly.

It was demonstrated in the present work that hydrophobic gold nanorods fabricated 2- and/or 3-D assemblies including the standing nanorod array, depending on the nanorod concentration. On the other hand, it has been reported that water-dispersed gold nanorods formed organized assemblies on a solid substrate or at the liquid–liquid interface.^{16,32,33} The longitudinal axes of such hydrophilic gold nanorods were parallel to the substrate or interface in every case. The assemblies of nanorods or nano-obelisks in a perpendicular arrangement were created by techniques such as chemical vapor deposition or lithography.³⁴ Consequently, the present paper concentrates on the formation of the standing gold nanorod array by a simple self-assembling process through evaporation of a solvent.

There is a report that CdSe nanorods ($3.7 \text{ nm} \times 18 \text{ nm}$) formed an ordered assembly in dispersion.³⁵ As far as we know, this study is only a trial on the structural estimation of a 3-D ordered nanorod assembly by SAXS. However, although arcs corresponding to the transversal spacing were observed, diffraction arcs originating from longitudinal spacing were not detected. This is due to the nematic arrangement of CdSe nanorods, where the array along the longitudinal direction is less. In the present work, the longitudinal ordering of gold nanorods was confirmed as described previously. This implies that the gold nanorods form a smectic-like ordered assembly in the solid state differently from the case of CdSe nanorods in the nematic dispersion.

Conclusion

In the present work, the preparation of hydrophobic gold nanorods was demonstrated by using organosilanes (MPS and ODS). This method provided an easy way for the hydrophobation of nanorods, the shell of which was chemically stable and thin. The obtained hydrophobic ODS-modified nanorods fabricated highly organized assemblies. The arrangement of the gold nanorods in the assemblies was controllable by the nanorod concentration. At a medium concentration, the gold nanorods formed a 2-D assembly where they were arranged parallel to the substrate via a side-by-side interaction. On the other hand, at a high concentration, another type of 2-D assembly was formed, that is, the nanorods stood on the substrate. At a solid state of gold nanorods, it was confirmed that the nanorods formed a 3-D assembly, where the gold nanorods were arranged in a hexagonal close-packed structure by their side-by-side interaction and the hexagonal arrays accumulated in a lamellar structure. The present discovery of hexagonal arrays and their accumulation as well as standing nanorods has never been reported before as far as we know.

Assembly formation by hydrophobic gold nanorods will create new possibilities for novel functionalities based on their anisotropic structure. Thus, as the next step, the investigation and discovery of "hot" properties such as optical, electrical, and mechanical behavior are required.

Acknowledgment. K.M. thanks the 21st COE Programs (Programs 14COEB01-00 and 14COEB012-00) in Nagoya University for financial support.

References and Notes

- Alivisatos, A. P. Semiconductor clusters, nanocrystals, and quantum dots. *Science* **1996**, *271*, 933–937.
- Tsuji, M.; Hashimoto, M.; Nishizawa, Y.; Kubokawa, M.; Tsuji, T. *Chem.—Eur. J.* **2005**, *11*, 440–452.
- Xiong, Y.; Wiley, B.; Chen, J.; Li, Z.-Y.; Yin, Y.; Xia, Y. *Angew. Chem., Int. Ed.* **2005**, *44*, 7913–7917.
- Shankar, S. S.; Rai, A.; Ahmad, A.; Sastry, M. *Chem. Mater.* **2005**, *17*, 566–572.
- Wang, L.; Chen, X.; Zhan, J.; Chai, Y.; Yang, C.; Xu, L.; Zhuang, W.; Jing, B. *J. Phys. Chem. B* **2005**, *109*, 3189–3194.
- Chandran, S. P.; Chaudhary, M.; Pasricha, R.; Ahmad, A.; Sastry, M. *Biotechnol. Prog.* **2006**, *22*, 577–583.
- Hirano, C.; Imae, T.; Yanagimoto, Y.; Takaguchi, Y. *Polym. J.* **2006**, *38*, 44–49.
- Wang, D.; Imae, T. *Chem. Lett.* **2006**, *35*, 1152–1153.
- Luo, X.; Imae, T. *J. Mater. Chem.* **2007**, *17*, 567–571.
- Kim, F.; Song, J. H.; Yang, P. *J. Am. Chem. Soc.* **2002**, *124*, 14316–14317.
- Chen, C.; Lin, Y.; Wang, C.; Tzeng, H.; Wu, C.; Chen, Y.; Chen, C.; Chen, L.; Wu, Y. *J. Am. Chem. Soc.* **2006**, *128*, 3709–3715.
- Takahashi, H.; Niidome, Y.; Niidome, T.; Kaneko, K.; Kawasaki, H.; Yamada, S. *Langmuir* **2006**, *22*, 2–5.
- Liz-Marzán, L. M. *Langmuir* **2006**, *22*, 32–41.
- Niidome, Y.; Urakawa, S.; Kawahara, M.; Yamada, S. *Jpn. J. Appl. Phys.* **2003**, *42*, 1749–1750.
- Jana, N. R.; Gearheart, L. A.; Obare, S. O.; Johnson, C. J.; Edler, K. J.; Mann, S.; Murphy, C. J. *J. Mater. Chem.* **2002**, *12*, 2909–2912.
- Jana, N. R. *Angew. Chem., Int. Ed.* **2004**, *43*, 1536–1540.
- Sau, T. K.; Murphy, C. J. *Langmuir* **2005**, *21*, 2923–2929.
- Chang, S.; Shih, C.; Chen, C.; Lai, W.; Wang, C. R. C. *Langmuir* **1999**, *15*, 701–709.
- Niidome, Y.; Nishioka, K.; Kawasaki, H.; Yamada, S. *Chem. Commun.* **2003**, 2376–2377.
- Sau, T. K.; Murphy, C. J. *Langmuir* **2004**, *20*, 6414–6420.
- Yang, J.; Wu, J.; Wu, Y.; Wang, J.; Chen, C. *Chem. Phys. Lett.* **2005**, *416*, 215–219.
- Pastoriza-Santos, I.; Pérez-Juste, J.; Liz-Marzán, L. M. *Chem. Mater.* **2006**, *18*, 2465–2467.
- Pérez-Juste, J.; Correa-Duarte, M. A.; Liz-Marzán, L. M. *Appl. Surf. Sci.* **2004**, *226*, 137–143.
- Blaudez, D.; Bonnier, M.; Desbat, B.; Rondelez, F. *Langmuir* **2002**, *18*, 9158–9163.
- Park, H. K.; Ha, T. H.; Kim, K. *Langmuir* **2004**, *20*, 4851–4858.
- Onoshima, D.; Imae, T. *Soft Matter* **2006**, *2*, 141–148.
- Yang, P.; Kim, F. *Chem. Phys. Chem.* **2002**, *3*, 503–506.
- Li, M.; Schnablegger, H.; Mann, S. *Nature* **1999**, *402*, 393–395.
- Manna, A.; Imae, T.; Yogo, T.; Aoi, K.; Okazaki, M. *J. Colloid Interface Sci.* **2002**, *256*, 297–303.
- Thomas, K. G.; Barazzouk, S.; Ipe, B. I.; Joseph, S. T. S.; Kamat, P. V. *J. Phys. Chem. B* **2004**, *108*, 13066–13068.
- Sudeep, P. K.; Joseph, S. T. S.; Thomas, K. G. *J. Am. Chem. Soc.* **2005**, *127*, 6516–6517.
- Nikoobakht, B.; Wang, Z. L.; El-Sayed, M. A. *J. Phys. Chem. B* **2000**, *104*, 8635–8640.
- Sau, T. K.; Murphy, C. J. *Langmuir* **2005**, *21*, 2923–2929.
- Galoppini, E.; Rochford, J.; Chen, H.; Saraf, G.; Lu, Y.; Hagfeldt, A.; Boschloo, G. *J. Phys. Chem. B* **2006**, *110*, 16159–16161.
- Li, L.; Alivisatos, A. P. *Adv. Mater.* **2003**, *15*, 408–411.